

CHAPTER 3

Sparsity based thresholding criterion for spurious echo removal and denoising MR spectra using rational-dilation wavelet transform

Chapter Highlights

- *Application of RADWT wavelet transform for denoising*
- *Peak estimation from denoised spectra of important metabolites*
- *Testing application over different spectra: Denoising of Raman Spectra*

3.1. Introduction:

The presence of noise and signal contamination (especially spurious echoes or spikes) due to internal systems or external environmental sources are inherent in any signal acquisition system. Overlapping of echoes over metabolite peaks poses a serious challenge in the accurate quantification of the metabolite information[3]. Therefore, denoising remains a prerequisite and is essential to every signal processing and analysis method. The basic objective of denoising is to improve the qualitative as well as the quantitative information for reliable and accurate analysis of a signal spectrum by reducing the effect of noise and artifacts.

Previously, traditional denoising methods have used either time domain or frequency domain-based analysis. Fourier transform (FT) and its variants have been used as global transformation functions for signal analysis, but are regarded inadequate in many cases related to singularities or non-stationary signals. The short time-frequency transform (STFT) method, incorporating the short-term window function, also does not meet the requirements. The introduction of wavelet transform (WT) as an alternative has opened a new paradigm in the field of signal processing. The seminal works of Daubechies[4] in filter design and that of Mallat[5] in the

development of efficient algorithms for discrete WTs created a platform for the current advances in wavelet-based signal processing[6].

The introduction of wavelets has significantly helped in resolving the problems associated with the non-stationary signals. WT provides multiresolution, time-frequency scale analysis and it can deal with the breakdown points and discontinuities in the higher derivatives. Like traditional high-pass and low-pass filtering, wavelet transform decomposes a signal into 'detail' and 'approximation' coefficient levels. A significant feature of wavelet transform is the dimension reduction of given datapoints using orthogonal bases and hence, presenting a sparse representation of data. Sparsity in decomposed wavelet coefficients of a signal can be exploited for denoising by applying an appropriate thresholding method[7]. Since most of the real biological signals have high redundancy, wavelet analysis using sparsity as an index of threshold determination can be utilized as a denoising methodology for signals.

3.2. Theory

3.2.1. Rational-Dilation Wavelet Transform (RADWT): This wavelet transform belongs to a family of over-complete, rational dilation-based (i.e., non-dyadic) transforms[8]. Unlike most of the existing over-complete WTs, where over-completeness is attained only by increasing the temporal sampling in frequency bands, overcomplete RADWTs increase sampling both in time and frequency bands providing different redundancy factors and better resolution of the signal. The implementation of this transform is based on an FFT-based filter bank which provides greater design flexibilities and can be utilized to generate several wavelet attributes that is difficult to realize with FIR filter-bank-based transforms. An array of Q-factors, frequency resolution and redundancy factors are achievable with this family of WT.

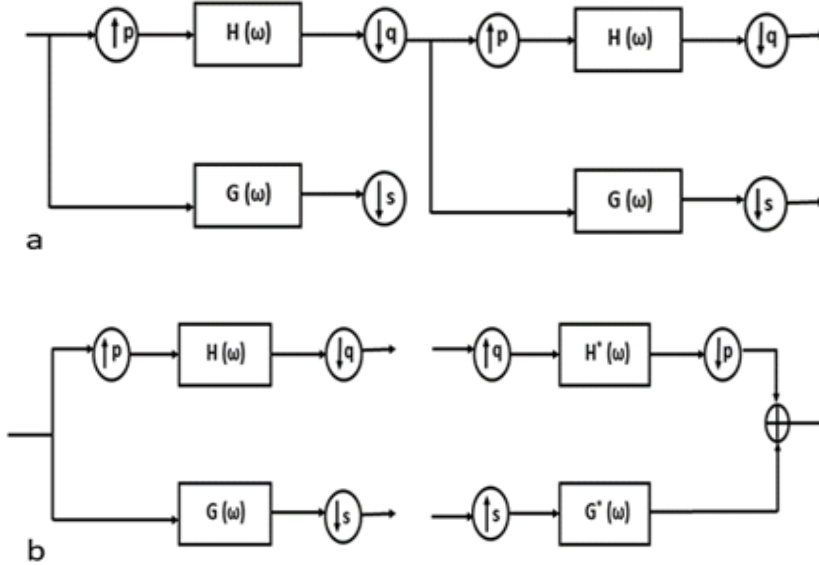


Figure 3.1 (a) Iterated filterbank for RADWT; (b) Analysis and Synthesis part of filterbank

The iterated filter bank for RADWTs is realized as depicted in Figure 3.1(a), whereas the analysis and synthesis part of the filter bank for the family of RADWT is represented in Figure 3.1(b), where, $H(\omega)$ and $G(\omega)$ are low pass and high pass filters respectively, satisfying perfect reconstruction (PR) conditions; p , q and s are constant +ve integers and the Dilation factor is represented as q/p , a rational number). The redundancy factor of the wavelet transform [8] is calculated as:

$$\text{Red}(p, q, s) = \frac{1}{s} \frac{1}{1 - \frac{p}{q}} \quad (3.1)$$

For $p = 7$, $q = 8$, and $s = 3$, the dilation factor = $8/7 \approx 1.14$ and Redundancy, $\text{Red}(p, q, s) = 8/3 \approx 2.67$. Using these parameters, the wavelet generated resembles a Gabor function and approximates a Gaussian-like shape (cosine function multiplied with a Gaussian function), which is similar to the MRS signal line shape. It is optimally localized in the time-frequency plane, has a high Q-factor with no ringing effects as shown in Figure 3.2 (a), (b), and (c).

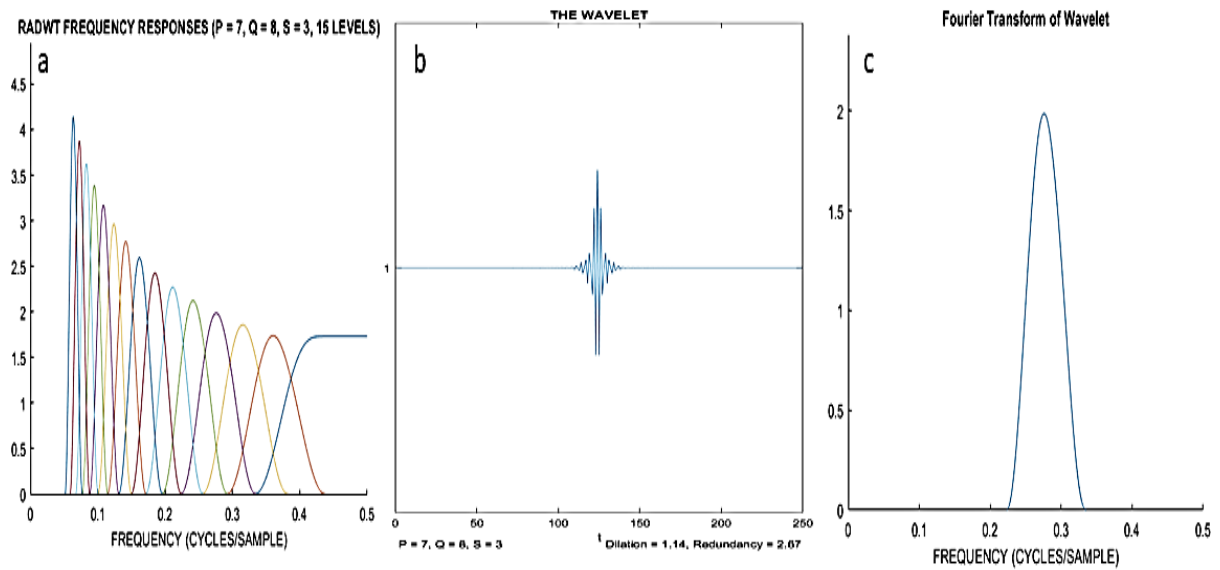


Figure 3.2: (a) RADWT frequency response of each of 15 levels of decomposition; (b) wavelet function resembling ‘Gabor’ function; (c) Fourier transform of wavelet function having Gaussian-like shape.

In this study, the performance of the above-mentioned overcomplete transform is investigated for denoising the MR spectroscopy signals. This family of wavelet transforms, designed for the discrete-time data, is a slightly overcomplete rational dilation-based (so non-dyadic), near shift-invariant and is self-inverting (tight-frame). For the compound MR spectra of individual metabolites with different relaxation times, this family of the tight frame wavelet transforms is expected to perform better as it gives the flexibility to vary frequency resolution and Q-factor, as required.

3.2.2. Sparsity measures ($L_{p,q}$ norm): Among different measures to calculate sparsity, norm-based measures have interesting benefits. $L_{p,q}$ norm is a generalized form of matrix norm expressed as:

$$L_{pq} = \left(\sum_{j=1}^n \left(\sum_{i=1}^m (|a_{ij}|^p) \right)^{\frac{q}{p}} \right)^{\frac{1}{q}} \quad (3.2)$$

For a vector of n data points, $A = (a_1, \dots, a_n)$, the matrix form is represented as $A = (a_{ij})$ such that $i = 1, \dots, m$ denotes summation over spatial dimension and $j = 1, \dots, n$ denotes the summation of data points. For $p = 2$, $q = 1$, $L_{2,1}$ norm[9] is given as:

$$L_{2,1} = \sum_{j=1}^n \left(\sum_{i=1}^m (|a_{ij}|^2) \right)^{\frac{1}{2}} \quad (3.3)$$

Here, the spatial domain attributes are measured in L_2 -space and data points summation is done over L_1 -space. $L_{2,1}$ norm, which behaves as an error function, is robust and is used in sparse coding where L_1 norm can be used to enforce sparsity as a penalty term on model parameters. In the current study, a modified form of $L_{2,1}$ norm is used which is expressed as[10] to calculate the sparsity of each wavelet decomposition level, j .

$$L_{2,1} = A_j = \frac{(\sum_{i=1}^n (|a_{ji}|^2))^{\frac{1}{2}}}{\sum_{i=1}^n (|a_{ji}|)} \quad (3.4)$$

Before wavelet decomposition of MR spectra into different levels, some specific steps of pre-processing are necessary to be performed, to prepare it for further analysis. These are:

1. Frequency alignment: FID is transformed into a frequency domain, and NAA singlet peak (located at 2.01 ppm) has been used as the reference to shift the overall spectra[11], [12].
2. Phase correction: To improve frequency-domain spectral analysis and quantitation, zero-phased correction is required. This correction is performed by multiplying a

complex phase factor from the initial points of FID with the complete complex spectrum[13], [14].

3. Eddy current correction (ECC): Due to switching of magnetic field gradients, eddy currents are produced according to Faraday's law of induction. During signal acquisition, a water unsuppressed signal along with a water suppressed signal is acquired following the same protocol. The correction is performed using the Klose method[15] by pointwise dividing the phase of the unsuppressed signal from the water suppressed signal.
4. Residual water peak suppression: During acquisition, signals are collected using CHESS or a similar sequence in an acquisition protocol to suppress the water resonance which is usually 10^3 to 10^4 times larger than the study-related metabolites. Despite suppression, there remains a residual water peak comparable to metabolite peaks in the signal. Hankel Singular value decomposition (HSVD) method has been used to remove these residual water peaks from the signal[16], [17].

Frequency alignment, Phase correction and residual water correction were performed using the jMRUI software platform[18] and ECC was performed on MATLAB.

Wavelet-based denoising is based on the idea of thresholding the decomposed levels obtained by transforming the original data using appropriate wavelets which would resemble the actual signal to obtain better noise separation. For the present study, the chosen wavelet resembles the Gabor function by manipulating the RADWT filter bank parameters as explained above.

The criteria of the sparsity measure to select the decomposition level have been chosen to be less than 0.1 of the level.

The process of denoising is implemented in the following way:

1. Signal Acquisition from the MR scanner.

2. Performing frequency alignment, phase correction, ECC, and residual water removal.
3. Addition of the noise to the signal.
4. Decomposition of the signal using RADWT into detailed and approximation levels.
5. Since decomposition levels have both +ve and -ve coefficients and contribute equally to noise and signal, the maximum of each +ve and -ve set of coefficients are obtained.
6. Thresholding criteria are applied to the coefficients and hard thresholding operation is used to delineate the signal coefficients from the noise coefficients.
7. Reconstruction is performed using inverse RADWT using the thresholded coefficients.

3.3. Thresholding criteria:

3.3.1. Existing methods: The decision of an accurate threshold is important to signal denoising. For values too small, there will be a considerable amount of noise remaining in the signal, and for values too large, some signal features might also get removed. Thresholding a wavelet coefficient for denoising was first proposed by Donohue[19], which used a fixed noise threshold for the decomposition levels. Also termed the universal threshold, it is calculated as

$$\lambda = \sigma \sqrt{2 \ln(N)} \quad (3.3)$$

where N is the signal length or decomposition level length and σ is the standard deviation of noise given by[20]

$$\sigma = \frac{\text{median}(|Y_{ij}|)}{0.6745} \quad (3.4)$$

Stein's Unbiased Risk Estimate (SURE) threshold, Minimax threshold[21] are some widely used and better performing fixed threshold estimates. Based on wavelet shrinkage[17], [22]–[27]; wavelet coefficient modelling [28], and modulus maxima[29]; many denoising methods have been developed with performances better than the conventional filtering operation[30].

Further, considering different properties of wavelet decomposition coefficients, different approaches of thresholding criteria have been proposed[31-35]. The idea of adaptive thresholding[22], [36] has evolved from the limitations of fixed thresholding methods like a) same noise threshold for each coefficient of a decomposition level without considering its bias and b) inability to discriminate between the coefficients when magnitudes of signal and noise coefficients are close. The above-mentioned issues are practically visible when analyzing a real experimental signal. Srivastava et al.[37] proposed a denoising method for adaptive noise threshold selection depending on the decomposition levels selected with application on cw-ESR spectra and presented promising results.

3.3.2. Proposed criteria

MR spectra are the combination of different chemical metabolite profiles of tissues resonating at frequencies slightly different from one another based on their local environments. The spectrum obtained is complex and the presence of noise and spurious echoes make denoising a challenging task. The method proposed by Srivastava et al. [37] is promising but is limited in maintaining individual peak morphology given the nature of MR spectra, which shows considerable differences in individual peak characteristics.

In the present work, an adaptive thresholding criterion is proposed where RADWT and $L_{p,q}$ -norm sparsity measure is employed to determine the decomposition levels and the threshold calculation for each decomposition level. The proposed method is implemented in the following way:

1. The signal is decomposed into detailed and approximation levels.
2. Sparsity measure A , of each detailed coefficient level is calculated and for levels having value for $A > 0.1$, the decomposition level is selected up to which wavelet decomposition. The cut-off value for A was chosen based on minimum reconstruction

loss in waveform by selecting decomposition levels with different values of A ranging between 0.001 to 0.5.

3. To cover all the +ve and -ve coefficients of the decomposition level, $\max|w_j > 0|$ and $\max|w_j < 0|$ are obtained.
4. On each subset for a decomposition level, the thresholding criteria is applied as:

$$\lambda_{j,L} = M_j - \alpha_{j,L}(M_j - \max|w_j < 0|) \quad (3.5.1)$$

$$\lambda_{j,H} = M_j + \alpha_{j,H}(M_j - \max|w_j > 0|) \quad (3.5.2)$$

5. Hard thresholding function is applied to remove the noisy coefficients from the signal components.
6. Using these coefficients, inverse RADWT is performed to reconstruct the denoised signal.

Here, $\lambda_{j,L}$ and $\lambda_{j,H}$ represents thresholds for -ve and +ve coefficients at the decomposition level j , respectively. M_j is the median and w_j is the wavelet coefficient of decomposition level j . In the present work, the median of the coefficients is considered, as it gives a better representation of the data when there is a possibility of a small proportion of extremely large or small value in the data, providing the most resistant statistic to these events. The presence of spikes or echoes is expected to generate wavelet coefficients of such nature. α_j is defined as a level-dependent parameter, using A calculated each decomposition level j , to adjust threshold values and is defined as:

$$\alpha_j = \left(1 - \frac{A_j}{A_r}\right) \quad (3.6.1)$$

where the reference sparsity level: $A_r = \frac{A_j + A_{j+1}}{2}$ (3.6.2)

3.3.3. Thresholding function: In the proposed method, a hard thresholding function was used on the noise thresholded coefficients for the accurate separation of the noise from the signal

coefficients. Combining the hard thresholding with the proposed thresholding criterion, the function is implemented as:

$$\tilde{w}_{j,i} = \begin{cases} 0 & : \quad \lambda_{j,L} \leq w_{j,i} \leq \lambda_{j,H} \\ w_{j,i} & : \quad \textit{otherwise} \end{cases} \quad (3.7)$$

where, $\tilde{w}_{j,i}$ is the noise thresholded wavelet coefficient at decomposition level j .

3.4. Method:

The eventual goal of denoising a medical signal is to obtain a better feature representation for the accurate quantitation and subsequently classification for diagnostic purposes. The use of the wavelet transform-based thresholding approaches for denoising is not new and different thresholding criteria have been presented in scientific kinds of literature since Donoho et al[19]. MR spectra generate complex-valued data with artifacts of varying characteristics depending upon the internal MR system as well as external environmental factors. The existing approaches are relatively efficient and sometimes aggressive in reducing the noise, causing distortions in the shape and envelop of the original MR spectra. The novel approach presented in this paper utilizes the flexibility of RADWT filters for better sparse representation of the signal and $L_{p,q}$ -norm-based index to capture the sparsity for effective thresholding to reduce the noise while maintaining the structure of the original signal. This is important for accurate feature-based studies and analysis and can also be used as inputs to machine learning classifiers for further analysis and inferences subjected to diagnostic purposes.

3.4.1. Dataset used:

MRS: All MR signals acquired are water suppressed free induction decay (FID) ^1H single-voxel spectroscopy (SVS) signals of the human brain at a magnetic field strength of 1.5 T Magnetom Avanto (Version BV-I7A; Siemens Medical System, Erlangen, Germany) with PRESS pulse sequence, at echo time $TE = 35$ ms and repetition time, $TR = 1500$ ms. The number of data points in the FID is 1024. A total number of 249 signals dataset (38 with tumor, 211 normal) has been obtained. The dataset used for this study is retrospective, hence the requirement of patient's consent was waived by the Institute Ethical Committee. 8 data signals (6 healthy, 2 tumor) were discarded on the ground of corruption of the prominent peaks in the signal because of the large artifacts due to patient movements, and the dataset of 241 signals (36 tumor and 205 normal spectra in the dataset) were used in the study.

A water unsuppressed FID with a similar protocol is also acquired for the eddy current correction.

Raman Spectroscopy: To examine the range of application and generalizability of the proposed method, the present method is also applied to the signals ($N=5$) acquired from the Raman spectroscopy data bank at the present Institute instrumentation facility and are also retrospective.

3.4.2. Evaluation metrics:

SNR: To compare the level of noise present in a signal, a Signal-to-noise ratio (SNR) is used. It is calculated by taking the ratio of summed squared magnitude of the signal and the noise.

$$SNR = \frac{\sum_{i=1}^N (x_i)^2}{\sum_{i=1}^N (x_i - \bar{x})^2} \quad (3.8)$$

RMSE: Root mean-squared error is a measure to show the amount of deviation of the residual error between the original and the reconstructed signal. It is calculated as:

$$RMSE = \sqrt{\frac{\sum_{i=1}^N (x_i - \tilde{x}_i)^2}{N}} \quad (3.9)$$

In (3.8) and (3.9), x_i is the original signal, \tilde{x}_i is the reconstructed signal after denoising, $(x_i - \tilde{x}_i)$ is the cumulative noise removed (additive white gaussian, random noise components, spike/echo components, small reconstruction error component) and $i = 1, \dots, N$ are the data points of the signal.

SSIM: Structural similarity index[38] is an objective measure commonly used in comparing the structural quality of images before and after processing in signals. The reconstructed signal can be compared with the original signal for structural similarity. In this study, the focus is maintained on the spurious echo removal along with the overall denoising of the signal, and therefore, SSIM was expected to be in the range of 0.85 to 0.95. It is calculated as:

$$SSIM (X, Y) = \frac{(2\mu_X\mu_Y + c_1)(2\sigma_{XY} + c_2)}{(\mu_X^2 + \mu_Y^2 + c_1)(\sigma_X^2 + \sigma_Y^2 + c_2)} \quad (3.10)$$

Here, the denoised signal is represented as X and the original signal as the reference signal Y; μ_X and μ_Y are the mean and σ_X and σ_Y are the standard deviation of X and Y respectively; σ_{XY} is the covariance of X and Y; c_1 and c_2 are stabilizing constant term, each for mean and standard deviation.

Peak Amplitude: MR spectra contain peaks specific to metabolites present in the tissues under study. The position of peaks and their amplitudes are essentially the most important feature for accurate quantification of metabolites and subsequent diagnosis.

The operation of the thresholding on the signal wavelet coefficients can alter the peak amplitudes when reconstructed. Therefore, the peak amplitude of a specific metabolite at its position before and after the denoising operation has been measured to test the perfect

reconstruction of the present method. NAA peak at 2.01 ppm, Cr peak at 3.01 ppm, and Cho peak at 3.21 ppm are taken as reference peaks to compare the measurement.

3.5. Experiments

1. In the first study, RADWT decomposition and the thresholding with different criteria, existing as well as proposed, was applied on MRS signals to evaluate the peak amplitude variations on the dataset of 241 MRS signals. Table 3.1 shows the mean values of the normalized amplitudes of NAA, Cr, Cho peaks after denoising.
2. In the second study, different thresholding methods were applied on MR signals containing spurious echoes near a peak to evaluate their ability to remove spurious echoes. Wavelet scattering transform was used on each of the denoised signals to obtain a scattergram coefficient matrix to compare the elimination of the spurious echoes from the signal. Scalograms plotting was done for the visualization of the echo component from the signal. Figure 3.3 (a-d) clearly shows that the present method can remove the echo component more effectively compared to the other methods. Although, for very low SNR spectra where noise amplitudes are comparable to low amplitude metabolite peaks, it may require further tuning of the wavelet parameters or use additional algorithmic aids for improved and efficient peak detection and isolation of smaller peaks. Some of the methods used to enhance the peak isolation in MRS have been presented in next chapters.
3. In the third study, the efficiency of the proposed method in overall denoising of the signal was evaluated by (Table 3.2), (i) without adding any additional noise to the signal, and then (ii) adding additive white gaussian noise to obtain noisy signals of 10 dB, 20 dB, 30 dB, 50 dB values. The parameter indices calculated for the comparison were SNR, RMSE and SSIM. Since the proposed method is based on an overcomplete rational-dilation based wavelet transform which is non-dyadic, denoising using Double

density dual-tree DWT (DDTDWT) [39][40], a dyadic transform method, has been performed for comparison. A thresholding method proposed by [37] was also implemented for denoising.

4. Finally, 5 test Raman signals were selected and the denoising was performed by adding the additive white gaussian noise of 25 dB to evaluate the efficacy of the proposed method for the different experimental or biological signals.

3.6. Results and Discussion:

The assessment of an effective signal denoising method cannot be just limited to the increase in the SNR factor. The abilities to differentiate between the weak signal components, maintaining the peak features like the amplitude and artifact correction are equally important.

Table 3.1: Comparison of Peak amplitudes after denoising using different thresholds

| Peak amplitude | NAA (2.01 ppm) | Cr (3.02 ppm) | Cho (3.21 ppm) |
|-----------------------|-----------------------|----------------------|-----------------------|
| Before Denoising | 0.6304 | 0.5823 | 1.000 |
| Method in [37] | 0.5998 | 0.5708 | 1.005 |
| Minimax-Hard | 0.614 | 0.5703 | 1.027 |
| Minimax-Soft | 0.5828 | 0.5623 | 0.946 |
| SURE-Hard | 0.6214 | 0.5718 | 1.015 |
| SURE-Soft | 0.6071 | 0.5701 | 0.9838 |
| Proposed | 0.6284 | 0.5799 | 0.9983 |

Table 3.2: Comparison results of different methods for denoising efficiency

| | SNR (dB) | RMSE | SSIM |
|-----------------|-----------------|----------------|---------------|
| Noisy Signal | 25.5682 | 0.00925 | 0.9164 |
| DDDT-DWT | 26.3170 | 0.01268 | 0.8791 |
| Method in [37] | 27.2768 | 0.00948 | 0.9523 |
| Proposed | 30.4193 | 0.00345 | 0.9604 |

Considering the above factors, three different experiments have been designed in the present study.

1. In the first study, different thresholding criteria were applied on RADWT decomposition coefficients and the reconstructed signals were compared to the peak amplitudes of NAA, Cr, and Cho. The complete dataset of 241 MR signals was used in this study and each signal was normalized before denoising, by dividing the signal by its maximum amplitude. In the table 3.1, the mean amplitude of 36 signals with the tumor cases has been shown where the Cho peak is used as the normalization peak. Similar results were obtained for the normal case signals where the NAA peak was taken as the normalization peak.

From the results obtained from this study, it is observed that the reconstruction using the proposed method of denoising is the closest to maintaining the peak amplitude of the signal.

2. In this study, 7 signals containing spurious echoes were chosen from the dataset. Spurious echoes result from the local susceptibility variations or insufficient spoiler gradient power during the acquisition. These echoes may overlap the metabolite peaks

causing incorrect estimation of peak areas and therefore concentration. On the signals with the spurious echoes embedding the signal, the proposed method of using the Gabor function like wavelet for decomposition was effective in eliminating the spurious echoes as shown in Fig 3.3. Other methods of thresholding were also tested using DWT with standard thresholds and the thresholding method proposed by [37]. To visualize the effectiveness of each method, 1st order scattering transform matrix of the denoised signals were calculated, and scalograms were plotted with the signal:

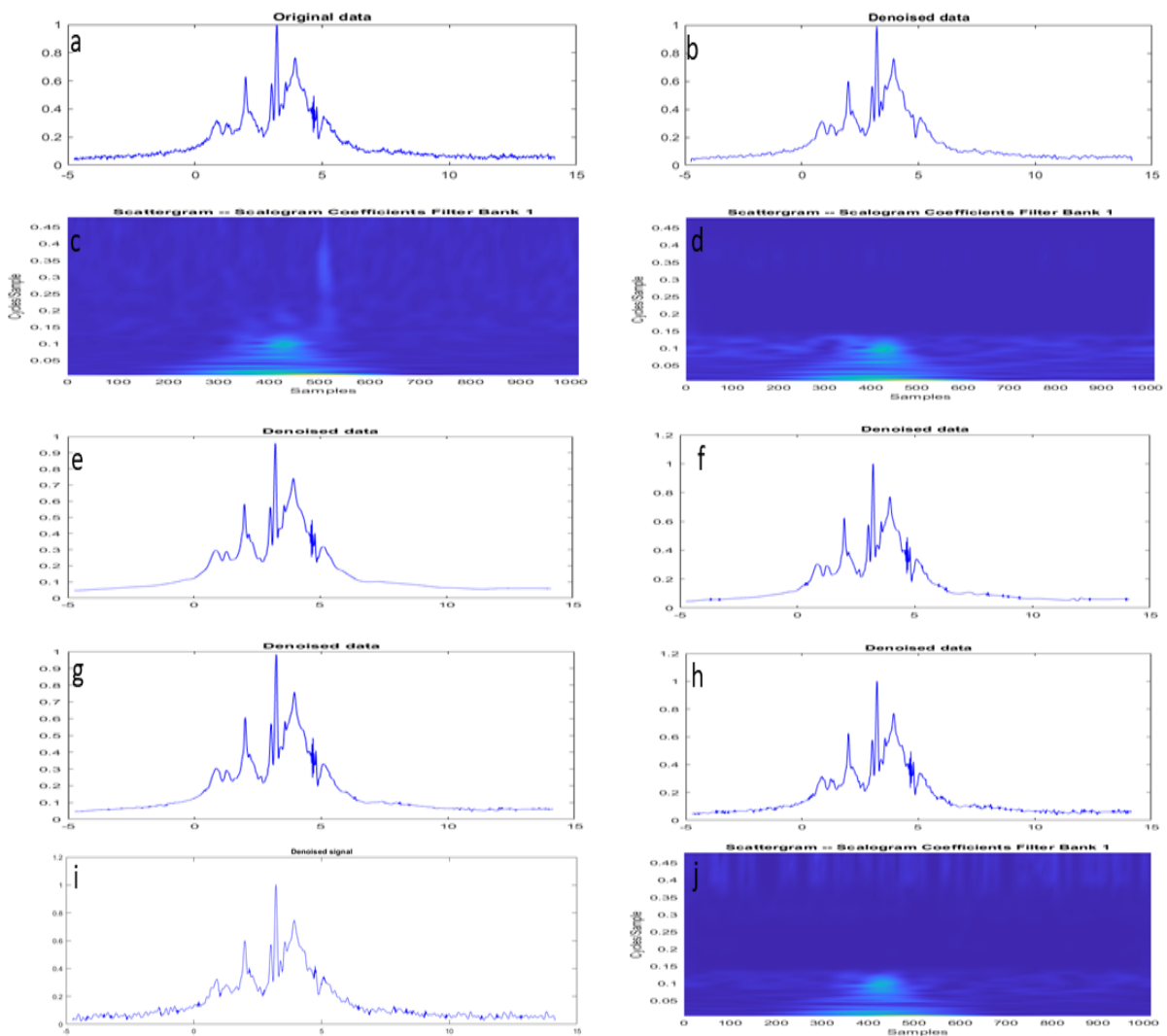


Fig 3.3: Visualization of spurious echo removal for comparison of different existing approaches: (a) Original signal with spurious echo; Spurious echo removal plot using different methods: (b) proposed method signal plot, (c) and (d) scalogram plot of (a) and

(b); (e) using Minimax-soft thresholding, (f) using Minimax hard thresholding, (g) using SURE-soft thresholding, (h) using SURE hard thresholding, (i) using Srivastava et al. method signal plot, (j) corresponding scalogram plot.

From the above comparisons, it can be deduced that although standard state-of-the-art methods render significant denoising effects, there are some morphological issues related to the denoised signals. It is observed in the signal plots that the denoised signals using the standard thresholds led to extra smoothing of the peaks, especially weak signals. Also, none of these methods were able to eliminate spurious echo components from the signal. The method proposed by [37] was able to reduce the echo component from the signal but not completely.

From the above two studies, it was concluded that the present method is better at handling artifacts while maintaining the peak amplitudes after the reconstruction of the MR signal. It can therefore be inferred that for the experimental biological signals which contain discontinuities and the weak signal components, the performance of the discussed method is significantly better.

In this study, the denoising efficiency of the proposed method was evaluated by calculating the SNR, RMSE and SSIM. After analyzing the performance of existing methods in the above studies, most of them were eliminated for further assessments. Therefore, for comparison, denoising was performed using the DDDT-DWT method and method proposed in [37] only, as they performed better in the previous two studies. For this study, denoising was performed on the complete dataset of 241 signals (7 spurious echoes containing signals as well) and adding additive white gaussian noise. The SNR, RMSE, and SSIM for the noisy signal were 25.5682 dB, 0.00925, and 0.9164 respectively. After denoising using three different methods on 241 signals, the evaluated parameter index values shown in Table 3.2 are the mean values over all signal outputs.

Similar experiments were also performed after adding the noise of 30 dB, 40 dB, and 50 dB and the results follow a similar pattern. Hence, it is concluded that the present method is efficient in denoising while maintaining the peak features of signals as supported by the parameter indices for evaluation. The calculated standard deviations of these indices for 241 signals are 0.7615, 0.0017, and 0.0181 for SNR, RMSE and SSIM respectively which further implies the stability and specificity of the proposed method for different noisy signals.

The Raman test signals were used to evaluate the application of the proposed method on the other experimental signals. With 25 dB of additive white gaussian noise added, the SNR, RMSE, SSIM values obtained were 32.8997, 0.0031, and 0.9684 respectively after denoising.

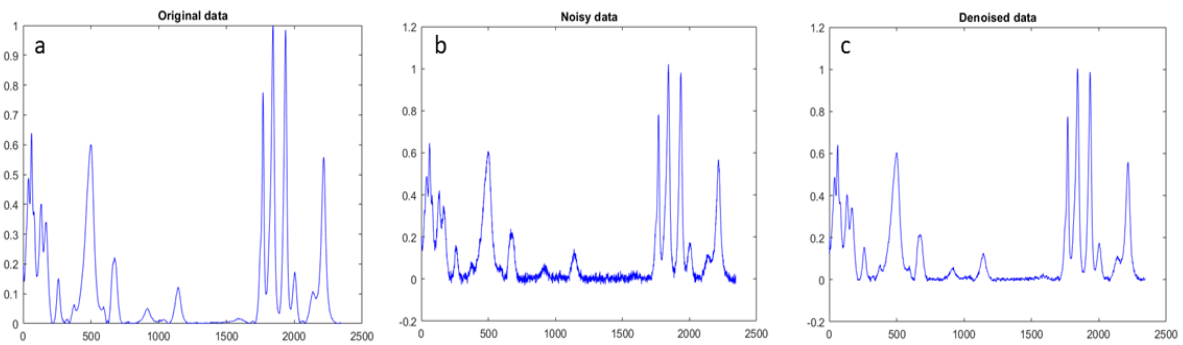


Figure 3.4: Denoising of Raman test signal by the proposed method

3.7. Conclusion

With the method proposed in this paper, it is shown that the denoising of signals is effective in terms of gain in SNR values, removal of the unwanted artifacts such as spurious echoes without distorting the peak characteristics of the spectra. This approach of denoising has been designed with the prospects of using the wavelets as feature extractors to be fetched as inputs to neural networks and machine learning architectures for further MRS study, and the results shown above are promising for further analysis. The flexibility in time-frequency resolution or choice of wavelet function using RADWT helps in sparser feature representation of signal which can

be used as input to different available classifiers directly to further obtain the most robust and specific analysis.

Besides MR spectra, the proposed method has also been applied on Raman spectroscopy signals showing improved outcomes. Therefore, it can be inferred that other than MRS, the present method also finds its application in denoising different biological or experimental signals.

Publication out of this study:

DOI 10.1007/s10812-022-01393-7

Journal of Applied Spectroscopy, Vol. 89, No. 3, July, 2022 (Russian Original Vol. 89, No. 3, May–June, 2022)

**SPARSITY-BASED THRESHOLDING CRITERION
FOR SPURIOUS ECHO REMOVAL AND DENOISING
MAGNETIC RESONANCE SPECTRA
USING RATIONAL-DILATION WAVELET TRANSFORM**

Ch. Sagar,^{a,*} D. Kumar Singh,^b and N. Sharma^a

UDC 543.422.23